

**1 Realistic initiation and dynamics of the**  
**2 Madden-Julian Oscillation in a coarse resolution**  
**3 aquaplanet GCM**

R. S. Ajayamohan,<sup>1</sup> Boualem Khouider<sup>2</sup> and Andrew J. Majda<sup>1,3</sup>

---

<sup>1</sup>Center for Prototype Climate Modelling,  
New York University, Abu Dhabi, UAE.

Email: Ajaya.Mohan@nyu.edu

<sup>2</sup>Department of Mathematics and  
Statistics, University of Victoria, BC,  
Canada.

<sup>3</sup>Courant Institute of Mathematical  
Sciences, New York University, USA

4 The main mechanisms for the initiation and propagation of the Madden-  
5 Julian Oscillation (MJO) are still widely debated. The capacity of operational  
6 global climate models (GCMs) to correctly simulate the MJO is hindered by  
7 the inadequacy of the underlying cumulus parameterizations. Here, we show  
8 that a coarse resolution GCM, coupled to a simple multcloud model param-  
9 eterization mimicking the observed dynamics and physical structure of or-  
10 ganized tropical convection, simulates the MJO in an idealized setting of an  
11 aquaplanet without ocean dynamics. We impose a fixed non-homogeneous  
12 sea surface temperature replicating the Indian Ocean/Western Pacific warm  
13 pool. This results in a succession of MJOs with realistic phase speed, am-  
14 plitude, and physical structure. Each MJO event is initiated at a somewhat  
15 random location over the warm pool and dies sometimes near the eastern  
16 boundary of the warm pool, and sometimes at a random location way be-  
17 yond the warm pool. Also occasionally the MJO events stall at the center  
18 of maximum heating. This is reminiscent of the fact that in nature some MJOs  
19 stall over the maritime continent while others reach the central Pacific Ocean  
20 and beyond. The initiation mechanism in the model is believed to be a com-  
21 bination of persistent intermittent convective events interacting with observed  
22 large scale flow patterns and internal tropical dynamics. The large scale flow  
23 patterns are associated with planetary scale dry Kelvin waves that are trig-  
24 gered by preceding MJO events and circle the globe while congestus cloud

25 decks on the flanks of the warm pool are believed to force Rossby gyres which  
26 then funnel moisture towards the equatorial region.

## 1. Introduction

27 The Madden-Julian Oscillation [*Madden and Julian, 1971*] is the dominant feature of  
28 the intraseasonal (20-100 days) variability in the tropical atmosphere. The MJO is an  
29 eastward propagating large-scale planetary scale disturbance in atmospheric winds and  
30 precipitation with coherent signals in many other variables. The MJO waves originate  
31 over the warm waters of the Indian Ocean (IO) and propagate eastward towards the  
32 maritime continent and Pacific Ocean with a speed of  $\approx 5\text{ms}^{-1}$ . The MJO interacts with  
33 the underlying oceans and influences the global weather and climate system [*Zhang, 2005*].

34 In spite of recent intensive research efforts [*Zhang, 2005; Lau and Waliser, 2005*], ac-  
35 curately simulating and predicting the MJO using state-of-the-art GCMs remains chal-  
36 lenging. Several missing links in understanding the physics and dynamics of the MJO  
37 have motivated co-ordinated efforts in observational and diagnostic studies in the last few  
38 years [*Zhang, 2005; Zhang et al., 2013*]. Realistic simulation of the observed phase and  
39 amplitude of the MJO is the most common bias seen in the climate model simulations.  
40 When eastward propagating MJOs are simulated, they are either too weak, or their spa-  
41 tial distributions and seasonal cycles are unrealistic [*Sligo et al., 1996; Lin et al., 2006;*  
42 *Straub et al., 2010; Kim et al., 2009*]. It is also noted that marked improvements have been  
43 made by few GCMs in simulating a realistic MJO [*Subramanian et al., 2011; Del Genio*  
44 *et al., 2012; Benedict et al., 2013; Crueger et al., 2013*].

45 Here, we use an aquaplanet model with a prescribed warm pool to simulate realistic  
46 MJOs. This model is designed without land or topography, without ocean-atmospheric  
47 coupling and without extratropical dynamics. In particular, a mask restricting heating

48 and cooling to the tropical belt between 30°S and 30°N is applied [see *Khouider et al.*,  
49 2011]. Here, we show that without boundary forcings and independent of initial condi-  
50 tions, a realistic simulation of MJO can be achieved. The main ingredient is the use of a  
51 simple-prototype multcloud model parameterization that is designed to capture the ob-  
52 served cloud morphology and dynamics of organized convection using three cloud types,  
53 congestus, deep, and stratiform, as the underlying building block [*Khouider and Ma-*  
54 *jda*, 2006a; *Khouider et al.*, 2011]. As opposed to traditional plume-based and large-scale  
55 forcing type parameterizations, the multcloud cloud model aims at representing the unre-  
56 solved mesoscale dynamics associated with organized convection which, by design captures  
57 the transition from shallow to deep convection through the progressive moistening due to  
58 congestus activity [*Khouider and Majda*, 2006a; *Mapes and Neale*, 2011; *Del Genio et al.*,  
59 2012].

60 The present study emphasizes primary mechanisms for the initiation and propagation of  
61 the MJO that are distinct from some other mechanisms presented in the literature. MJO  
62 initiation can be triggered due to a variety of mechanisms including chaotic reorganization  
63 of intermittent convective events by pre-existing large scale circulation patterns and/or  
64 the intrusion of extra-tropical disturbances in winds, temperature, and/or moisture. This  
65 interpretation is in essence compatible with the DYNAMO/CINDY [*Zhang et al.*, 2013]  
66 field campaign working hypothesis, stipulating the existence of both a dynamical (ex-  
67 ternal) and a convective (local) initiation of the MJO, which classifies MJO events into  
68 primary and successive categories [*Ling et al.*, 2013].

69 The paper is organized as follows. The diagnostics used in analyzing the results are  
70 described in Section 2. Discussion of the results and conclusions are outlined in Sec-  
71 tion 3. The description of the model and the experiment setup is outlined in the auxiliary  
72 material.

## 2. MJO Diagnostics

73 MJO-like characteristics are obtained from the numerical simulation of the Multi-  
74 cloud\_HOMME Model (MHM; details of model configuration and set up outlined in the  
75 auxiliary material). A Hovmöller (longitude-time) plot of the 200hPa zonal wind (U200;  
76 shaded) and precipitation (vertically averaged heating; PCP; contours) averaged over the  
77 equatorial belt 10°S-10°N is shown in Fig. 1. A succession of MJO-like events are clearly  
78 seen in both zonal winds and precipitation. They are formed over the warm pool and  
79 propagate slowly eastward at roughly  $5\text{ms}^{-1}$ . Before they die as they exit the warm pool  
80 region, these MJO-like signals trigger fast moving streaks of wind disturbances that con-  
81 tinue to move eastward but at a much faster speed of roughly  $25\text{ms}^{-1}$ , a second-baroclinic  
82 dry Kelvin wave. Dry Kelvin waves are believed to play an important role in the dy-  
83 namics and initiation of the MJO [Matthews *et al.*, 1999]. As they propagate and circle  
84 the globe, these waves act as a precursor for MJO initiation in MHM. They do so via  
85 the associated planetary scale divergence field that organizes the otherwise chaotic and  
86 intermittent mesoscale convective systems, represented by the multcloud model. This  
87 cause-and-effect interaction is confirmed by the magnified picture in Fig. 2.

88 To illustrate the characteristics of the simulated MJO, we carry out more diagnostics  
89 like wave-frequency spectra on the three variables U850, U200 and PCP [Wheeler and

90 *Kiladis*, 1999]. The wave-frequency spectra show peak variance in the MJO band in the  
91 period between 30 and 80 days and zonal wave number 1-2 (Fig. 3). Elevated variance  
92 over the Kelvin wave regime is also evident in Fig. 3. Another prominent MJO diagnostic  
93 is based on the coherency between these three variables by computing the Combined Em-  
94 pirical Orthogonal Function [CEOF; *Madden-Julian Oscillation Working Group*, 2009].  
95 An average of 20-100 day band pass filtered anomalies of PCP, U850 and U200 in tropics  
96 ( $15^{\circ}\text{S}$ - $15^{\circ}\text{N}$ ) is calculated. After normalizing each of these three fields separately by the  
97 square-root of the zonal mean of their temporal variance at each longitudinal point, a com-  
98 bined EOF of these three fields is computed. Based on a two dimensional phase diagram  
99 of first and second principal components (PC1 & PC2), eight different phases of the MJO  
100 are identified. The spatial composites of the selected points according to these phases  
101 show steady eastward propagation of MJO and associated spatial pattern in each phase  
102 (Fig. 4). The initiation of MJO over the warm pool (phase 4), slow eastward propagation  
103 over the warm pool region (phases 5-7), triggering of Kelvin waves and its propagation  
104 from the dateline (phases 8-3) is clearly evident in the composite spatial structure (Fig. 4),  
105 consistent with observations [*Madden-Julian Oscillation Working Group*, 2009].

106 In addition to the diagnostics presented here, the MJO-like wave simulated by the  
107 MHM has many other, if not all, the, principal features of the MJO as observed in nature,  
108 including the tilted baroclinic structure in zonal winds and temperature and a quadruple  
109 vortex structure (see auxiliary Fig.1) in the upper and lower troposphere surrounding the  
110 active convection [*Kiladis et al.*, 2009]. Another important feature of the MHM, is the

111 ability of congestus cloud decks on the flanks of the convective core to reinforce these  
112 Rossby gyres which, in turn, funnel moisture along the equator [*Khouider et al.*, 2011].

### 3. Summary and Discussion

113 Several theories for the genesis of the MJO have been proposed in the past [*Wang*,  
114 2005]. By the design of the multicloud model parameterization [e.g. *Khouider and Majda*,  
115 2006a] none of the following mechanisms are present in the simulation; Wind Induced  
116 Surface Heat Exchange (WISHE), wave-CISK (Convective Instability of the Second Kind),  
117 boundary layer friction (FCI), cloud radiation forcing (CRF), ocean/sea-surface dynamics.  
118 Nevertheless, the MHM produces MJO-like events with dynamical and physical features  
119 that resemble observed MJOs, including stochastic initiation over the warm pool and  
120 sudden demise after propagating the length of the warm pool and sometimes beyond.

121 The multicloud heating acts on high-frequency disturbances to produce instability,  
122 through across-scale interactions, adequate for the genesis and propagation of the MJO  
123 [*Khouider and Majda*, 2006a]. This concept is rooted on the observational evidence that  
124 the MJO and embedded disturbances involve the multicloud structure: a deep convective  
125 core preceded by shallow convection or congestus clouds and trailed by upper-tropospheric  
126 stratus clouds [*Johnson et al.*, 1999; *Mapes et al.*, 2006]. When properly coupled to mois-  
127 ture, a two vertical mode model, the first and second baroclinic modes, can generate  
128 instability sufficient to drive tropical waves [*Khouider and Majda*, 2006a, b]. The convec-  
129 tive activity coupled with large-scale circulation takes the form of an envelope of mesoscale  
130 and synoptic scale systems involving multiple cloud types [*Johnson et al.*, 1999; *Nakazawa*,  
131 1988].



132 Several studies accentuate the role of land in stalling the MJO to attain its slow phase  
133 speed [Matthews *et al.*, 1999]. The fact that the aquaplanet MHM simulates MJO-like  
134 events indicate the secondary influence of land on the MJO genesis. An important role  
135 of air-sea interaction and related ocean dynamics in simulating realistic phase and am-  
136 plitude of an MJO is highlighted in the ECHAM family of models [Crueger *et al.*, 2013].  
137 Moreover, baroclinic instability and extratropical connection are not present in the MHM  
138 simulations. The MHM results suggests that realistic MJOs in a GCM is possible without  
139 land, ocean dynamics, baroclinic instability and extratropical interaction. Our results ad-  
140 vocate that the primary factors responsible for the initiation of MJO differ entirely from  
141 most existing theories.

142 Our aquaplanet results show that MJO initiation can occur internally via the organi-  
143 zation of chaotic organized convective events above the warm pool involving a moisture-  
144 coupled mode of the tropical troposphere internal variability represented by the MJO-  
145 skeleton model [Majda and Stechmann, 2009, 2011; Kim *et al.*, 2013]. An opposing school  
146 of thought advocates a Kelvin-Rossby Gill-type coupling in lieu of the MJO-mode, in-  
147 volving no moisture coupling [Wang and Rui, 1990]. However, a drawback is that such a  
148 structure can not produce the observed quadruple vortex structure of the MJO. Earlier  
149 MJO theories rely on mechanisms such as WISHE, CRF, wave-CISK, and FCI to pro-  
150 duce instability. Moreover, the moisture mode instability advocated by Kim *et al.* [2013]  
151 has no scale selection property—all scales are unstable. The MJO acts as an envelope for  
152 mesoscale and synoptic scale convective systems, which in return, provide the necessary  
153 heating and upscale transport of momentum to sustain the MJO [Biello and Majda, 2005;

154 *Majda and Stechmann, 2009*]. In essence, across scale interactions and the existence of  
155 the embedded mesoscale and synoptic scale systems ensure the coupling between mois-  
156 ture and MJO dynamics. This is guaranteed by introducing a synoptic scale envelope of  
157 wave-activity in the neutrally stable MJO skeleton model [*Majda and Stechmann, 2009*].

158 The success of the multcloud model is rooted in its systematic use of mesoscale convec-  
159 tive system (MCS) dynamics as the building block for the dynamical coupling of congestus,  
160 deep, and stratiform heating profiles based on the first two baroclinic modes of vertical  
161 structure. In this fashion, unlike traditional cumulus parameterizations, parameterized  
162 convection is not confined into a single grid column and single time step but distributed  
163 over the length and time scales of the MCSs and synoptic scale systems embedded in the  
164 MJO, as demonstrated by linear theory [*Khouider and Majda, 2006a; Khouider et al.,*  
165 *2012*]. This is consistent with *Moncrieff* [2004], who successfully used a systematic rep-  
166 resentation of the MCS circulation patterns to overcome the vertical column pitfall of the  
167 underlying parameterization to drive convective momentum transport also addressed in  
168 the multiscale context by *Biello et al.* [2007].

## References

- 169 Benedict, J. J., E. D. Maloney, A. H. Sobel, D. M. Frierson, and L. J. Donner (2013), Trop-  
170 ical intraseasonal variability in version 3 of the GFDL atmosphere model, *J. Climate*,  
171 *26*, 426–449.
- 172 Biello, J., and A. J. Majda (2005), A multi-scale model for the Madden-Julian oscillation,  
173 *J. Atmos. Sci.*, *62*, 1694–1721.

- 174 Biello, J., A. J. Majda, and M. W. Moncrieff (2007), Meridional momentum flux in the  
175 multiscale IPESD MJO model, *J. Atmos. Sci.*, *64*, 1636–1651.
- 176 Crueger, T., B. Stevens, and R. Brokopf (2013), The Madden-Julian Oscillation in  
177 ECHAM6 and the introduction of an objective MJO metric, *J. Climate*, *26*, 3241–3256,  
178 doi:10.1175/JCLI-D-12-00413.1.
- 179 Del Genio, A. D., Y. Chen, D. Kim, and M.-S. Yao (2012), The MJO transition from  
180 shallow to deep convection in CLOUDSAT/CALIPSO data and GISS GCM simulations,  
181 *J. Climate*, *25*, 3755–3770, doi:10.1175/JCLI-D-11-00384.1.
- 182 Johnson, R. H., T. M. Rickenbach, S. A. Rutledge, P. E. Ciesielski, and W. H. Schubert  
183 (1999), Trimodal characteristics of tropical convection, *J. Climate*, *12*(8), 2397–2418.
- 184 Khouider, B., and A. J. Majda (2006a), A simple multcloud parameterization for con-  
185 vectively coupled tropical waves. Part I: Linear analysis, *J. Atmos. Sci.*, *63*, 1308–1323.
- 186 Khouider, B., and A. J. Majda (2006b), Model multi-cloud parameterizations for con-  
187 vectively coupled tropical waves: Detailed nonlinear wave evolution, *Dynam. Atmos.*  
188 *Oceans*, *42*, 59–80.
- 189 Khouider, B., A. St-Cyr, A. J. Majda, and J. Tribbia (2011), The MJO and convectively  
190 coupled waves in a coarse resolution GCM with a simple multcloud parameterization,  
191 *J. Atmos. Sci.*, *68*, 240–264, doi:10.1175/2010JAS3443.1.
- 192 Khouider, B., Y. Han, A. J. Majda, S. N. Stechmann (2012), Multiscale waves in an MJO  
193 background and convective momentum transport feedback, *J. Atmos. Sci.*, *69*, 915–933,  
194 doi:10.1175/JAS-D-11-0152.1.

- 195 Kiladis, G. N., M. C. Wheeler, P. T. Haertel, K. H. Straub, and P. E. Roundy  
196 (2009), Convectively coupled equatorial waves, *Rev. Geophys.*, *47*, RG2003, doi:  
197 10.1029/2008RG000266.
- 198 Kim, D., et al. (2009), Application of MJO simulation diagnostics to climate models, *J.*  
199 *Climate*, *22*(23), 6413–6436, doi:10.1175/2009JCLI3063.1.
- 200 Kim, D., J.-S. Kug, and A. H. Sobel (2013), Propagating vs. non-propagating Madden-  
201 Julian oscillation events, *J. Climate*, p. in press, doi:JCLI-D-13-00084.1.
- 202 Lau, W. K. M., and D. E. Waliser (Eds.) (2005), *Intraseasonal Variability in the*  
203 *Atmosphere-Ocean Climate System*, 474 pp., Springer, Heidelberg, Germany.
- 204 Lin, J.-L., et al. (2006), Tropical intraseasonal variability in 14 IPCC AR4 climate models.  
205 Part I: Convective signals, *J. Climate*, *19*(12), 2665–2690.
- 206 Ling, J., C. Zhang, and P. Bechtold (2013), Large-scale distinctions between MJO and  
207 non-MJO convective initiation over the tropical Indian ocean, *J. Atmos. Sci.*, *70*, 2696–  
208 2712, doi:JAS-D-13-029.1.
- 209 Madden, R. A., and P. R. Julian (1971), Detection of a 40-50 day oscillation in the zonal  
210 wind in the tropical Pacific, *J. Atmos. Sci.*, *28*, 702–708.
- 211 Madden-Julian Oscillation Working Group, C. (2009), MJO simulation diagnostics, *J.*  
212 *Climate*, *22*, 3006–3030, doi:10.1175/2008JCLI2731.1.
- 213 Majda, A. J., and S. N. Stechmann (2009), The skeleton of tropical intraseasonal oscilla-  
214 tions, *Proc. Nat. Acad. Sci. USA*, *106*(21), 8417–8422.
- 215 Majda, A. J., and S. N. Stechmann (2011), Nonlinear dynamics and regional variations  
216 in the mjo skeleton, *J. Atmos. Sci.*, *68*(12), 3053–3071, doi:10.1175/JAS-D-11-053.1.

- 217 Mapes, B., S. Tulich, J. Lin, and P. Zuidema (2006), The mesoscale convection life cycle:  
218 Building block or prototype for large-scale tropical waves?, *Dynam. Atmos. Oceans*, *42*,  
219 3–29, doi:10.1016/dynatmoce.2006.03.003.
- 220 Mapes, B. E., and R. B. Neale (2011), Parameterizing convective organization to escape  
221 the entrainment dilemma, *J. Adv. Model. Earth Sys.*, *3*, M06,004.
- 222 Matthews, A. J., J. M. Slingo, B. J. Hoskins, and P. M. Inness (1999), Fast and slow  
223 kelvin waves in the Madden-Julian oscillation of a GCM, *Quart. J. Roy. Meteorol. Soc.*,  
224 *125*, 1473–1498.
- 225 Moncrieff, M. W. (2004), Analytic representation of the large-scale organization of tropical  
226 convection, *J. Atmos. Sci.*, *61*(13), 1521–1538, doi:10.1175/1520-0469(2004)061<1521:  
227 AROTLO>2.0.CO;2.
- 228 Nakazawa, T. (1988), Tropical super clusters within intraseasonal variations over the  
229 western Pacific, *J. Meteorol. Soc. Japan*, *66*(6), 823–839.
- 230 Slingo, J. M., et al. (1996), Intraseasonal oscillation in 15 atmospheric general circulation  
231 models: Results from an AMIP diagnostic subproject, *Clim. Dynam.*, *12*, 325–357.
- 232 Sobel, A., and E. Maloney (2012), An Idealized Semi-Empirical Framework for Mod-  
233 eling the Madden-Julian Oscillation, *J. Atmos. Sci.*, *69*, 1691–1705, doi:10.1175/  
234 JAS-D-11-0118.1.
- 235 Straub, K. H., P. T. Haertel, and G. N. Kiladis (2010), An analysis of convectively coupled  
236 Kelvin waves in 20 WCRP CMIP3 global coupled climate models, *J. Climate*, *23*, 3031–  
237 3056, doi:10.1175/2009JCLI3422.1.

- 238 Subramanian, A. C., M. Jochum, A. J. Miller, R. Murtugudde, R. B. Neale, and D. E.  
239 Waliser (2011), The Madden-Julian oscillation in CCSM4, *J. Climate*, *24*, 6262–6282,  
240 doi:10.1175/JCLI-D-11-00031.1.
- 241 Wang, B. (2005), Theory, in *Intraseasonal Variability in the Atmosphere-Ocean Climate*  
242 *System*, edited by W. K. M. Lau and D. E. Waliser, chap. 10, pp. 307–360, Praxis  
243 Springer, Berlin.
- 244 Wang, B., and H. Rui (1990), Dynamics of the coupled moist Kelvin-Rossby wave on an  
245 equatorial beta-plane, *J. Atmos. Sci.*, *47*, 397–413.
- 246 Wheeler, M., and G. N. Kiladis (1999), Convectively coupled equatorial waves: Analysis  
247 of clouds and temperature in the wavenumber-frequency domain, *J. Atmos. Sci.*, *56*,  
248 374–399.
- 249 Zhang, C. (2005), Madden-Julian Oscillation, *Rev. Geophys.*, *43*, RG2003, doi:10.1029/  
250 2004RG000158.
- 251 Zhang, C., J. Gottschalck, E. Maloney, M. Moncrieff, F. Vitart, D. Waliser, B. Wang, and  
252 M. Wheeler (2013), Cracking the MJO nut, *Geophys. Res. Lett.*, doi:10.1002/grl.50244.

253 **Acknowledgments.** Center for Prototype Climate Modelling (CPCM) is fully funded  
254 by the Abu Dhabi Government through New York University Abu Dhabi (NYUAD) Re-  
255 search Institute grant. This research was initiated during an extended visit of B.K. and  
256 A.M. to the CPCM at NYUAD during winter 2012. The computations were carried out  
257 on the High Performance Computing resources at NYUAD and early tuning of the code  
258 were done at the University of Victoria using the West Grid computing Network. The  
259 research of BK is partially funded by the Natural and Engineering Research Council of  
260 Canada.

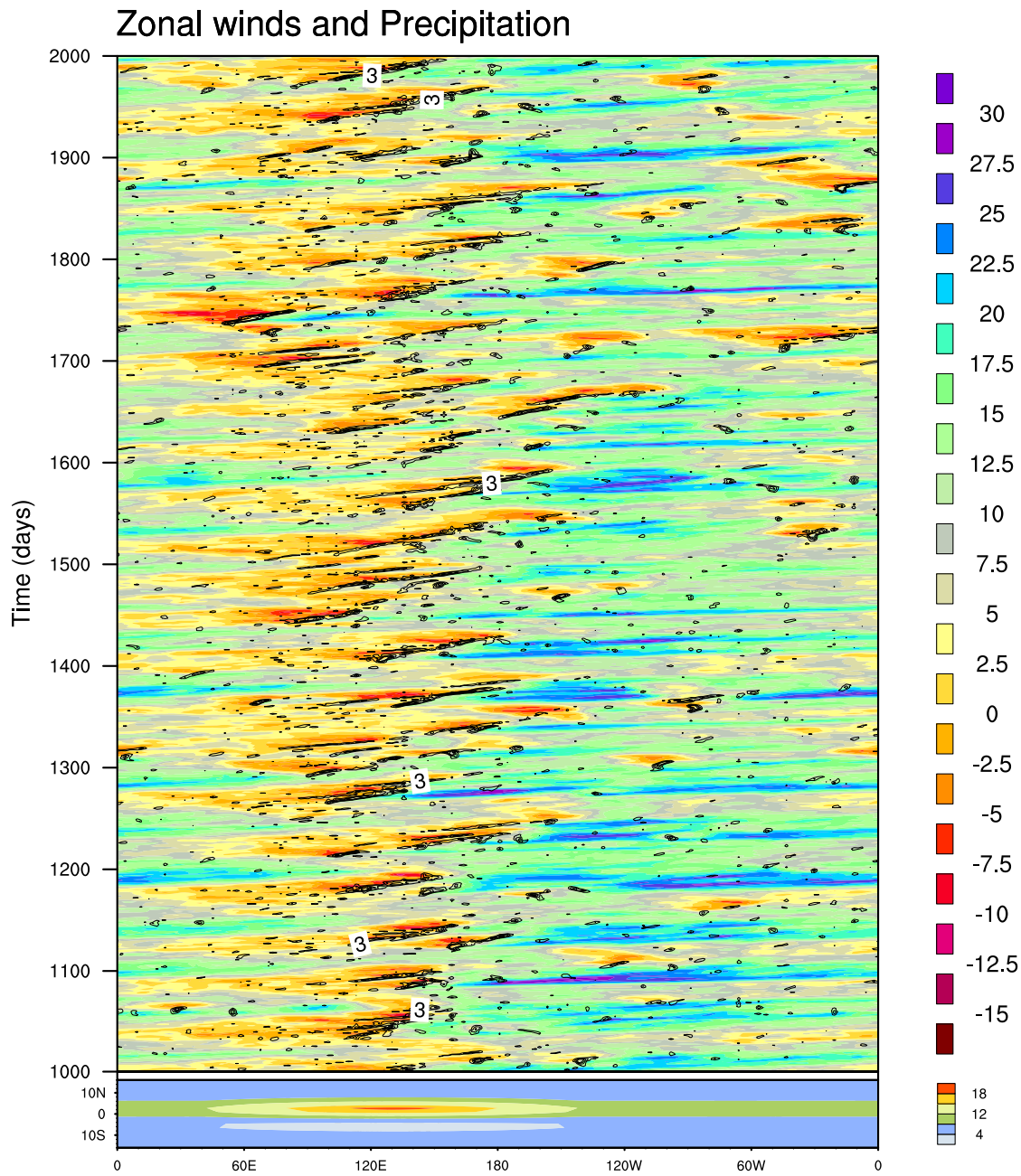


**Figure 1. Propagation of zonal winds and precipitation:** Hovmöller plot of upper level zonal winds (shaded,  $\text{ms}^{-1}$ ) and precipitation (contour,  $\text{K}\cdot\text{day}^{-1}$ ) averaged over the equatorial belt ( $10^{\circ}\text{S}$ - $10^{\circ}\text{N}$ ). Structure of the warm pool ( $^{\circ}\text{C}$ ) used in the simulations is shown in the bottom panel.



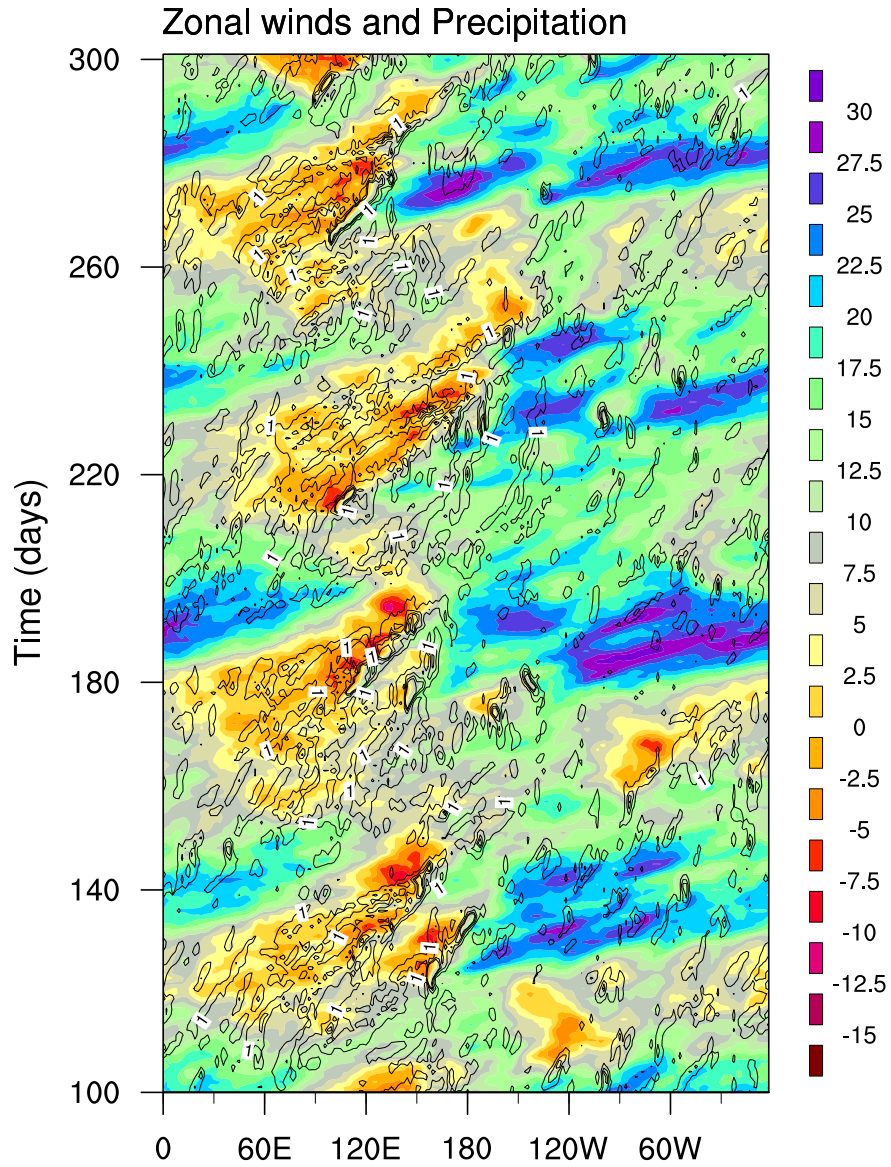


**Figure 2.** Propagation of zonal winds and precipitation: Same as Fig. 1 but zoomed during a short period. Starting contour is  $1 \text{ K}\cdot\text{day}^{-1}$  with an interval of  $3 \text{ K}\cdot\text{day}^{-1}$ .

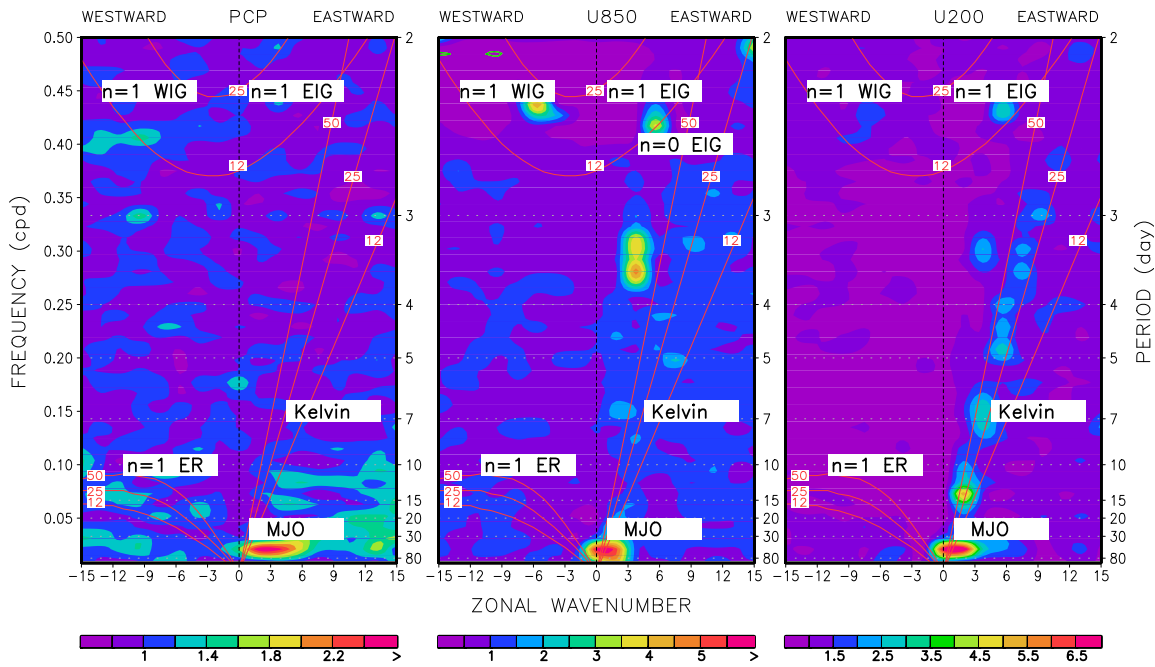


**Figure 3.** Wave-Frequency spectra of the symmetric component of precipitation, 850hpa winds and 200hPa zonal winds calculated for the last 1000 days from a 2000 days simulation. Time series is split into thirty 96 segments with a 65-day overlapping for smoothing.

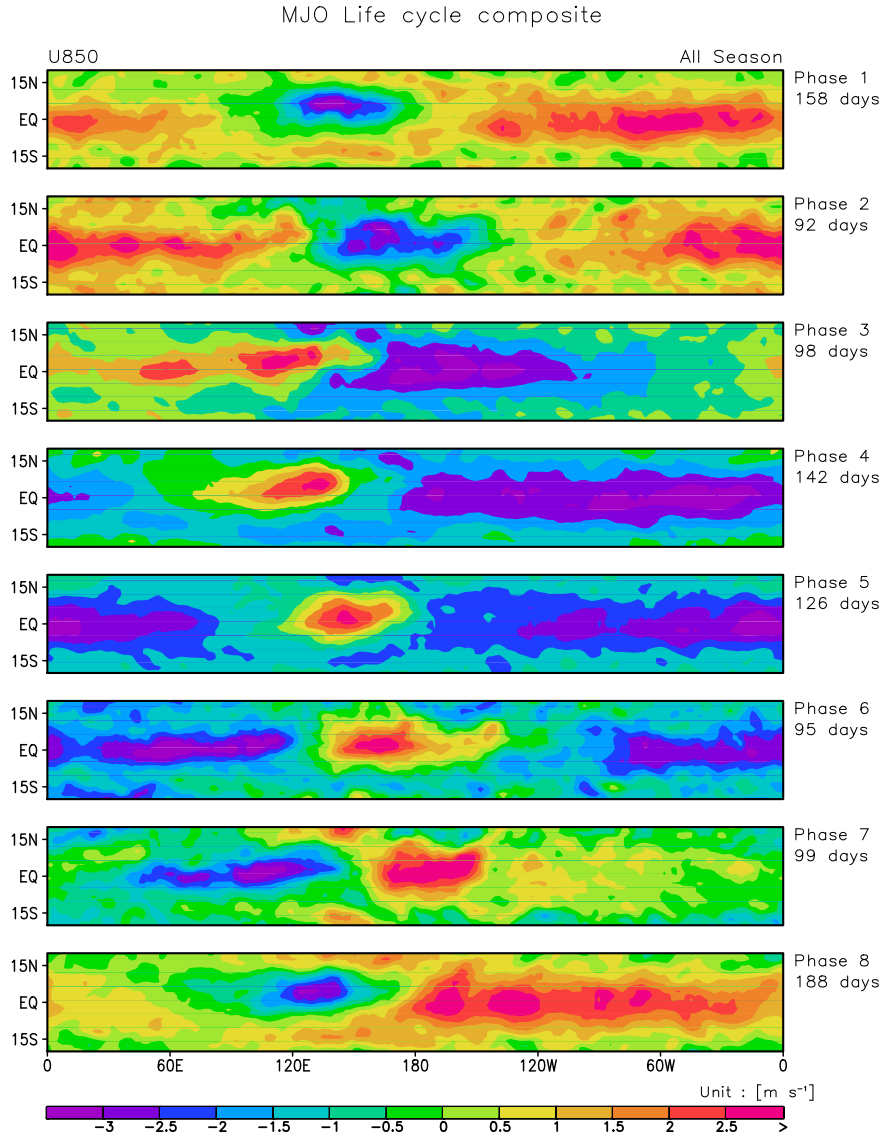


**Figure 4.** Life-Cycle composites of 850hPa zonal winds of the simulated MJO.

(a) Identify MJO events through plots of PC-1 vs. PC-2 from the combined EOFs. Specifically, select points exceeding a root-mean-square exceeding 1 [i.e.  $\sqrt{\text{PC-1}^2 + \text{PC-2}^2} > 1$ ]. (b) Based on a two dimensional phase diagram of PC-1 and PC-2, define eight different phases of the MJO and generate spatial composites of the selected points according to these phases.

## Auxiliary Material

### Model and Setup

The High-Order Methods Modelling Environment (HOMME) is a highly parallelized code based on spectral element discretization of the hydrostatic primitive equations developed by the National Center for Atmospheric Research (NCAR), USA [Dennis *et al.*, 2005; Nair and Tufo, 2007]. HOMME relies on a cubed-sphere grid, where the earth is tiled with quasi-uniform quadrilateral elements, free from polar singularities. Here, we run the HOMME model in coarse resolution as a dry dynamical core coupled to the multcloud parameterization [Khouider *et al.*, 2011]. The multcloud model assumes three heating profiles associated with the three cloud types, congestus, deep, and stratiform, that characterize tropical convective systems. These heating profiles force directly the first and second baroclinic modes of vertical structure. Mid-level moisture is used as a proxy to switch between congestus and deep convection regimes. When the midtroposphere is dry congestus clouds are favored and when it is moist deep convection is preferred. Stratiform heating trails deep convection by a prescribed time lag of 3 hours [Khouider and Majda, 2006]. Congestus clouds serve to moisten the mid-troposphere via the induced second baroclinic low-level convergence and precondition the environment for deep convection. The multcloud model is implemented in the full resolution Atmospheric General Circulation Model (AGCM) by invoking the vertical structure normal modes [Khouider *et al.*, 2011]. An asymmetric warm pool (Fig. 1; bottom panel) is forced over 60°E-180°E (roughly above Indo-W.Pacific region in a model with land) in this model setup. The AGCM is allowed to run freely for 2000 days;

outputs were collected for every six hours and the results of the last 1000 days were analyzed to avoid model spin-up.

## References

- Dennis, J., A. Fournier, W. F. Spitz, A. St-Cyr, M. A. Taylor, S. J. Thomas, and H. M. Tufo (2005), High-resolution mesh convergence properties and parallel efficiency of a spectral element atmospheric dynamical core, *International Journal of High Performance Computing Applications*, *19*(3), 225–235, doi:10.1177/1094342005056108.
- Khouider, B., and A. J. Majda (2006), A simple multcloud parameterization for convectively coupled tropical waves. Part I: Linear analysis, *J. Atmos. Sci.*, *63*, 1308–1323.
- Khouider, B., A. St-Cyr, A. J. Majda, and J. Tribbia (2011), The MJO and convectively coupled waves in a coarse resolution GCM with a simple multcloud parameterization, *J. Atmos. Sci.*, *68*, 240–264, doi:10.1175/2010JAS3443.1.
- Nair, R., and H. M. Tufo (2007), Petascale atmospheric general circulation models, in *Journal of Physics: Conference Series*, vol. 78, p. 012078, IOP Publishing, doi:10.1088/1742-6596/78/1/012078.

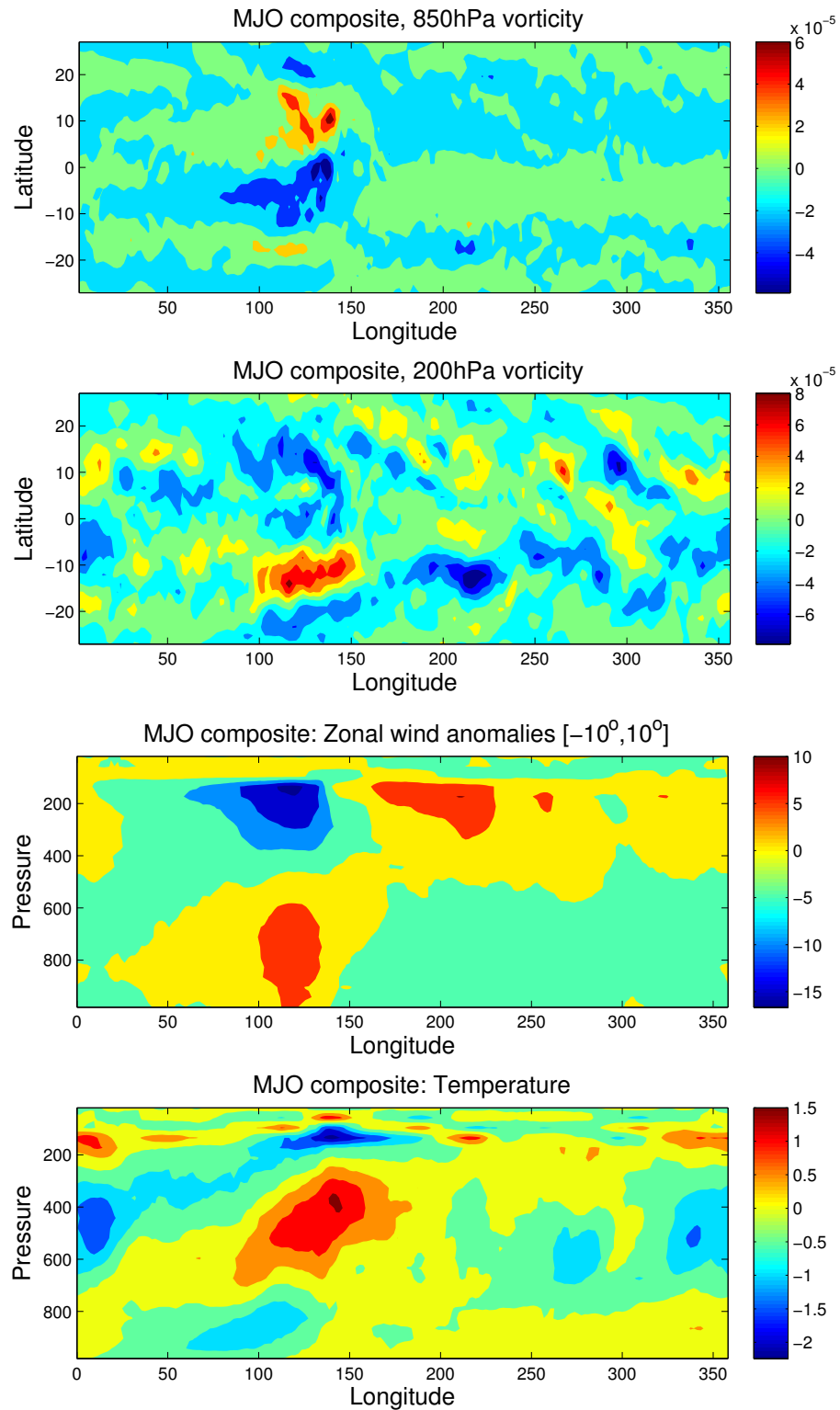


**Figure 1.** Horizontal and vertical structure of the MJO in MHM simulations.

MJO-filtered vorticity ( $\text{s}^{-1}$ ), zonal winds ( $\text{ms}^{-1}$ ) and temperature (K) anomalies are shown.